Discovery of Endothelial to Mesenchymal Transition as a Source for Carcinoma-Associated Fibroblasts

Elisabeth M. Zeisberg,[1] Scott Potenta,[1] Liang Xie,[1] Michael Zeisberg,[1] and Raghu Kalluri[1,2,3]

[1]Division of Matrix Biology, Department of Medicine, Beth Israel Deaconess Medical Center and Harvard Medical School; [2]Department of Biological Chemistry and Molecular Pharmacology, Harvard Medical School; and [3]Harvard-MIT Division of Health Sciences and Technology, Boston, Massachusetts

Abstract

Activated fibroblasts are associated with many different tumors. Myofibroblasts, activated fibroblasts, and perivascular mesenchymal cells such as pericytes play a role in cancer progression. Many studies suggest that myofibroblasts facilitate tumor growth and cancer progression. The source for myofibroblasts and other activated fibroblasts within the tumors is still debated. Although *de novo* activation of quiescent fibroblasts into α-smooth muscle actin (αSMA)–positive myofibroblasts is one likely source, epithelial to mesenchymal transition and bone marrow recruitment are also evolving as possible mechanisms for the emergence of a heterogeneous population of carcinoma-associated fibroblasts. Here, we show that transforming growth factor-β1 could induce proliferating endothelial cells to undergo a phenotypic conversion into fibroblast-like cells. Such endothelial to mesenchymal transition (EndMT) is associated with the emergence of mesenchymal marker fibroblast-specific protein-1 (FSP1) and down-regulation of CD31/PECAM. Additionally, we show EndMT in tumors using the B16F10 melanoma model and the Rip-Tag2 spontaneous pancreatic carcinoma model. Crossing *Tie2-Cre* mice with *R26Rosa-lox-Stop-lox-LacZ* mice allows for irreversible tagging of endothelial cells. We provide unequivocal evidence for EndMT at the invasive front of the tumors in these transgenic mice. Collectively, our results show that EndMT is a unique mechanism for the accumulation of carcinoma-associated fibroblasts and suggest that antiangiogenic treatment of tumors may have a direct effect in decreasing activated fibroblasts that likely facilitate cancer progression. [Cancer Res 2007;67(21):10123–8]

Introduction

Cancer research has traditionally focused on the alterations within genetically transformed cancer cells. In recent years, however, tumors have been increasingly perceived as complicated unorganized organs that, in addition to the cancer cells, also contain various stroma cells, such as endothelial cells, immune cells, and fibroblasts (1–3). In fact, in some carcinomas, >90% of the tumor consists of the stroma (4, 5). Stromal cells influence many aspects of tumor development including inception, growth, angiogenesis, local invasion, and metastasis (1, 2).

Although it is widely accepted that fibroblasts facilitate tumor progression, the origin(s) of such activated fibroblasts are largely unknown. Activated fibroblasts likely arise from several sources. Activation and proliferation of resident tissue fibroblasts contribute to fibroblast accumulation in the tumor microenvironment (1). Recent studies also point to a possible origin of carcinoma-associated fibroblasts (CAF) from the bone marrow. Moreover, periadventitial cells (including pericytes and vascular smooth muscle cells) are implicated as sources of activated fibroblasts (1).

Here, we explore a hypothesis that proliferating endothelial cells might contribute to CAF via endothelial to mesenchymal transition (EndMT). We show that in two different mouse models of carcinogenesis, EndMT contributes to the appearance of CAF. We further show that primary mouse endothelial cells acquire a fibroblast-like phenotype upon exposure to transforming growth factor-β1 (TGF-β1). Furthermore, we provide evidence that tumors in endothelial cell–specific *LacZ* reporter mice contain fibroblasts that are also *LacZ*$^+$. These results suggest that EndMT is also a source for the emergence of CAF in the tumor microenvironment.

Materials and Methods

Mice. C57BL/6 mice were from The Jackson Laboratory. Rip1-Tag2 mice were obtained from the National Cancer Institute Mouse Repository. Starting at 12 weeks of age, all RIP1-Tag2 mice received 50% sugar in their food (Harlan Teklad) to counteract hypoglycemia induced by the insulin-secreting tumors. *Tie2Cre* and *R26Rosa-lox-Stop-lox-LacZ* alleles were described previously (6, 7). The LacZ is designed to express under the control of the ROSA promoter. In the *Tie2Cre;R26Rosa-lox-Stop-lox-LacZ* double transgenic mice, the stop codon at the start of the lacZ coding sequence is deleted by Cre recombinase. *Tie2Cre* mice express the Cre recombinase in endothelial cells, therefore, the *lacZ* gene is also expressed in endothelial cells. To obtain *Tie2Cre;R26Rosa-lox-Stop-lox-LacZ* mice, matings were set-up between *Tie2* Cre-positive and homozygous *R26Rosa-lox-Stop-lox-LacZ* mice. These mice exhibit normal phenotypes and life spans. All mice were housed under standard conditions in the animal facility of the Beth Israel Deaconess Medical Center, Boston, MA. All experiments were conducted with the approval of the Institutional Animal Care and Use Committee of the Beth Israel Deaconess Medical Center.

Tumor studies. B16F10 cells were grown at 37°C in 5% CO_2 in DMEM with 10% heat-inactivated fetal bovine serum (FBS) and 5 ng/mL of plasmocin under sterile tissue culture conditions. The backs of C57BL/6 mice were shaved and B16F10 cells were injected s.c. on the backs of the mice (1×10^6 cells/mouse). The tumors were measured using Vernier calipers, and the volume was calculated using a standard formula (width^2 × length × 0.52; ref. 8). Tumors were harvested when they reached ~1,000 mm^3. The B16F10 melanoma model was used due to the expression of melanin in cancer cells. This provides an additional method to distinguish cancer cells from tumor-associated stromal cells.

Isolation of primary mouse lung endothelial cells. Mouse lung endothelial cells (MLEC) were isolated from 12-week-old wild-type C57BL/6 mice as described in our previous publications (9). Briefly, intracellular adhesion molecule-2 expressing MLEC were enriched using rat anti-mouse intracellular adhesion (molecule-2; PharMingen) conjugated to magnetic beads (Dynabeads M-450; Dynal). MLEC were maintained in 40% Ham's

Requests for reprints: Raghu Kalluri, Division of Matrix Biology, Department of Medicine, Harvard Medical School, Dana 514, Beth Israel Deaconess Medical Center, 330 Brookline Avenue, Boston, MA 02215. Phone: 617-667-0445; Fax: 617-975-5663; E-mail: rkalluri@bidmc.harvard.edu.

doi:10.1158/0008-5472.CAN-07-3127

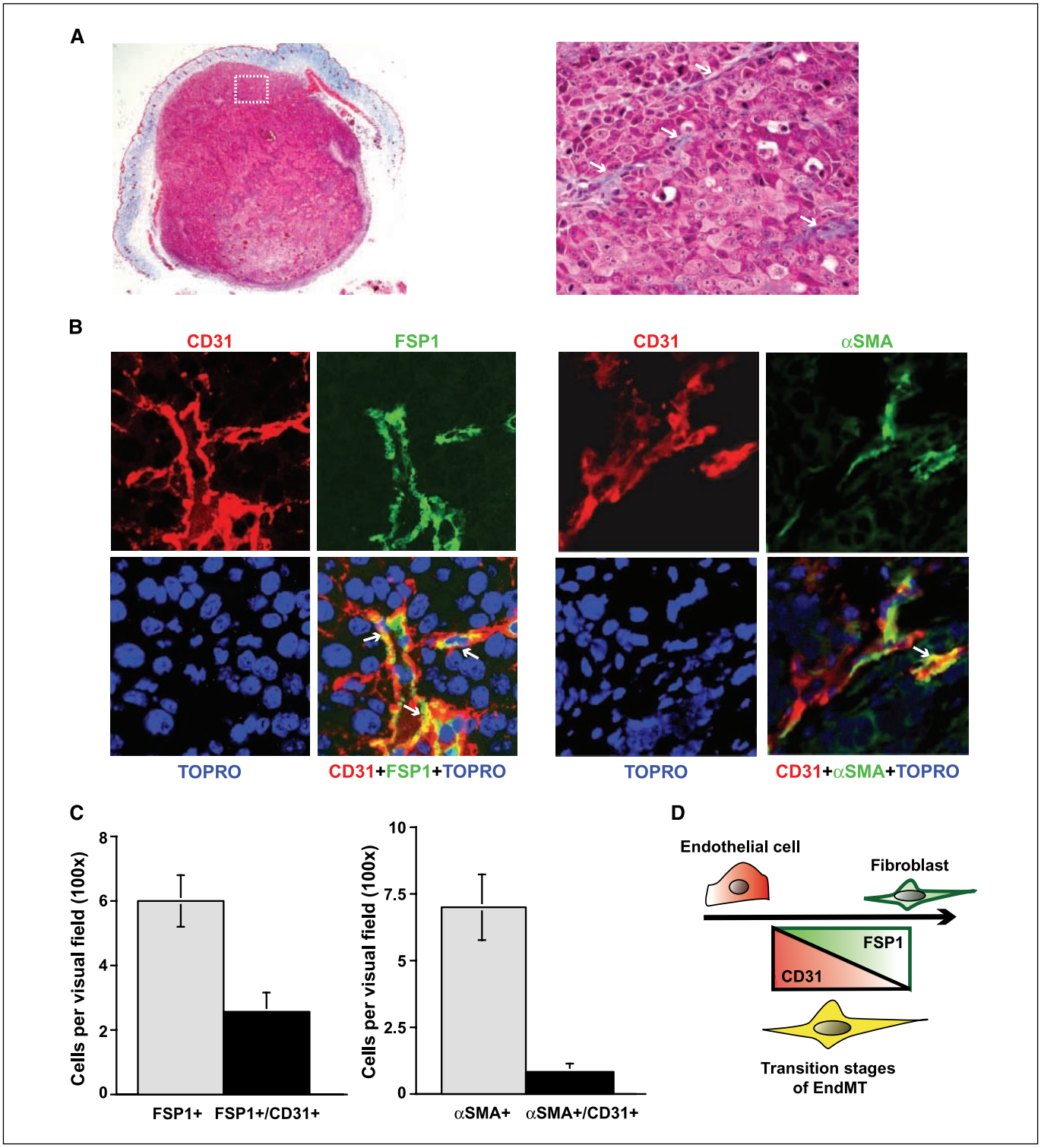

Figure 1. *A,* B16F10 subcutaneous tumors in C57BL/6 mice. B16F10 cancer cells were implanted s.c. into C57BL/6 mice. B16F10 tumors were analyzed when they reached a size of 800 to 1,000 mg. *Left,* a representative photomicrograph of an MTS-stained tumor section (original magnification, ×1.25). *Right,* inset from left (original magnification, ×40). Corresponding areas were analyzed by immunofluorescence labeling as displayed below. *B,* FSP1-CD31 and αSMA-CD31 double-labeling of B16F10 tumors. Confocal microscopy of cryosections double-labeled with antibodies to CD31 (*red, left*) and FSP1 (*green, left*) and to CD31 (*red, right*) and αSMA (*green, right*). TOPRO-3 was used for labeling of nuclei (*blue*). In addition to the single-color panels, the pictures were merged (*bottom right*). *Arrows,* cells which were labeled positive for both FSP1 and CD31 (*yellow, left*) or both αSMA and CD31 (*right*). Original magnification, ×100. *C, left,* the number of all FSP1-positive cells (*empty column*) and FSP1/CD31 double-positive cells (*filled column*) per visual field; *right,* the number of all αSMA-positive cells (*empty column*) and αSMA/CD31 double-positive cells (*filled column*) per visual field. *D,* schematic illustration. EndMT involves a progressive loss of endothelial cell markers (*CD31*) associated with a reciprocal gain of mesenchymal markers (*FSP1*). CD31 and FSP1 double-labeling allows for the identification of intermediate stages of EndMT *in vivo* ($CD31^+FSP1^+$), a complete conversion cannot be detected due to the likely total loss of endothelial markers in the newly emerged fibroblast-like cells.

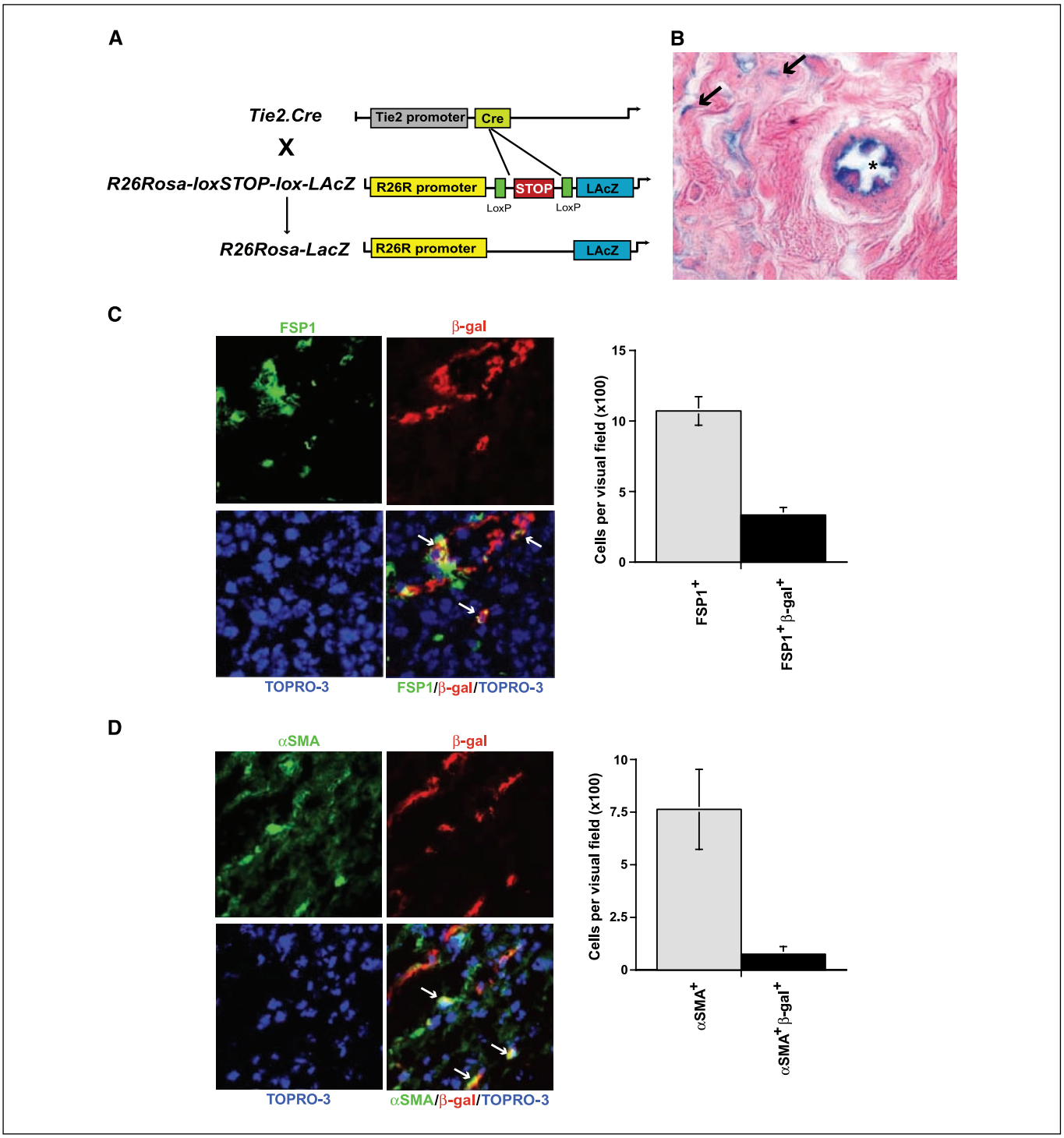

Figure 2. *A,* schematic illustration. To test for EndMT by endothelial cells, *R26Rosa-lox-STOP-lox* transgenic mice, in which the *LacZ* reporter gene is separated from the ubiquitously expressed Rosa26 promoter by a floxed stop (pgk.NEO) sequence, were crossed with mice transgenic for tie2.cre recombinase. The cre recombinase splices out the stop sequence in endothelial cells (unfloxed or LacZ+) in *R26Rosa-lox-STOP-lox* transgenic mice, irreversibly tagging the cells by LacZ expression irrespective of its phenotypic fate. EndMT-derived fibroblasts can be detected by means of β-galactosidase/FSP1 double-labeling, whereas fibroblasts that derive from resident FSP1$^+$ fibroblasts are positive for FSP1, but not β-galactosidase. *B,* β-galactosidase staining of a B16F10 tumor grown in a *tie2-cre;R26Rosa-loxstop-lox-lacz* transgenic mouse. Cells which expressed the tie2-cre transgene (indicative of their endothelial cell origin) in this assay (*blue*); *, a vessel in which endothelial cells stain positive; *arrows,* single cells which are dispersed in the tumor stroma (possible EndMT-derived fibroblasts). Original magnification, ×60. *C,* FSP1$^+$/β-gal$^+$ cells in B16F10 tumors. B16f10 tumor grown in a *tie2-cre;R26Rosa-loxSTOP-lox-lacz* transgenic mouse labeled with antibodies to β-galactosidase (*red*) and FSP1 (*green*). The representative pictures were obtained with a confocal microscope. *Arrows,* double-positive cells (*bottom right*). Nuclei were counterstained using TOPRO-3 (*blue*). Original magnification, ×100. *Columns,* number of all FSP1-positive cells (*empty column*) and FSP1/β-gal double-positive cells (*filled column*) per visual field. *D,* αSMA$^+$/β-gal$^+$ cells in B16F10 tumors. B16F10 tumor grown in a *tie2-cre;R26Rosa-loxstop-lox-lacz* transgenic mouse labeled with antibodies to β-galactosidase (*red*) and αSMA (*green*). The representative pictures were obtained with a confocal microscope. *Arrows,* double-positive cells (*bottom right*). Nuclei were counterstained using TOPRO-3 (*blue*). Original magnification, ×100. *Columns,* the number of all αSMA-positive cells (*empty column*) and αSMA/β-gal double-positive cells (*filled column*) per visual field.

F-12, 40% DME-low glucose, 20% FBS supplemented with heparin, endothelial mitogen (Biomedical Technologies, Inc.), glutamine, and penicillin/streptomycin. MLEC were characterized for homogeneity by morphologic observations and by immunofluorescence staining for endothelial-specific markers as previously described (9). Cells between passages 3 and 6 were used for the experiments.

***In vitro* induction of EndMT.** Primary MLECs (1×10^6/dish) were cultured in 40% Ham's F-12, 40% DME-low glucose, 2% FBS supplemented with heparin, glutamine, and penicillin/streptomycin once they had adhered. In order to induce EndMT, the medium was supplemented with 10 ng/mL of TGF-β1.

Immunocytochemistry. EndMT in MLEC was visualized by immunofluorescent double staining with antibodies to CD31, α-smooth muscle actin (αSMA), and fibroblast-specific protein-1 (FSP1) as described with minor modifications (10). Cells were fixed with acetone and incubated overnight at 4°C with the primary antibodies. Cells were then washed again and incubated for 45 min at room temperature with Alexa Fluor 488– and 568-conjugated secondary antibodies (Invitrogen). The cells were covered using Vectashield mounting media (Vector). Staining was analyzed using a confocal microscope.

Immunohistochemistry. We did immunohistochemistry as previously described (11). Frozen tissue was cut into 5-μm-thick cross-sections which were fixed in 100% acetone at −20°C for 10 min. We incubated the sections with primary antibodies at 4°C overnight. The primary antibodies were rat anti-CD31 (clone MEC13.3; BD PharMingen), mouse anti–αSMA (clone 1A4; Sigma), rabbit anti-FSP1 (polyclonal, research gift from Eric G. Neilson, Vanderbilt University, Nashville, TN), rabbit anti–β-galactosidase (polyclonal; Cappel), mouse anti-FSP1 (clone 1F12-1G7; Novus Biologicals). For detection of primary antibodies raised in rabbit or rat, we used Alexa Fluor 488– and 568–conjugated secondary antibodies (Invitrogen). Primary antibodies raised in mice were detected using the M.O.M. kit (Vector Laboratories). After the sections were washed with TBS, they were subsequently stained with secondary antibodies. The nuclei were counterstained with 4′,6-diamidino-2-phenylindole (Vectashield) for fluorescence microscopy or with TOPRO-3 (Molecular Probes) for confocal microscopy. FSP-1 antibody was a gift from E.G. Neilson. Staining was analyzed using a Zeiss LSM 510 Meta scanning confocal microscope. Ten visual fields per tumor and three size-matched (~1,000 mm^3) tumors were analyzed for colocalization of endothelial and fibroblast markers.

LacZ staining. Frozen tissue was cut into 5-μm-thick cross-sections which were fixed in 4% paraformaldehyde at 4°C for 10 min. Sections were then washed thrice in PBS and then incubated at 37°C in 1 mg/mL of X-Gal (Sigma), 5 mmol/L of potassium ferrocyanide, 5 mmol/L of potassium ferricyanide, 2 mmol/L of $MgCl_2$, 0.2% NP40, and 0.1% sodium-deoxycholate in PBS for 72 h as described (12).

Statistical analysis. Descriptive analysis was done using SigmaStat software. Results are expressed as means ± SE.

Results

$FSP1^+CD31^+$ and αSMA^+CD31^+ double-positive cells in B16F10 mouse melanomas. Previous studies show that EndMT contributes to the accumulation of fibroblasts in the setting of heart fibrosis, similar to EndMT which occurs during heart development (13). Here, we test the hypothesis that a portion of the fibroblasts present in the tumors could derive from endothelial cells via EndMT. We analyzed B16F10 mouse melanomas (Fig. 1*A*) and we did labeling experiments using antibodies to CD31 (endothelial cell marker; *red*) and the fibroblast markers FSP1 (*green*) and αSMA (*green*). Confocal microscopy reveals colocalization of both FSP1 and CD31 as well as of αSMA and CD31 (Fig. 1*B*). Approximately 11% of the αSMA^+ cells in the tumor microenvironment are double-positive for both αSMA and CD31. Among the $FSP1^+$ perivascular cells in the tumor periphery, ~40% were also labeled positive for CD31, suggesting that these cells represent a class of CAFs that also express endothelial markers (Fig. 1*C* and *D*).

LacZ and FSP1 double-positive cells in the tumor stroma of *Tie2-cre;R26Rosa-lox-Stop-lox-LacZ* transgenic mice. FSP1/CD31 and αSMA/CD31 double-labeling experiments using antibodies allow for the identification of intermediate stages of EndMT, but not for cells of endothelial cell origin that have lost their endothelial cell markers. Therefore, we did studies using implanted s.c. B16F10 tumors in *Tie2-cre;R26Rosa-lox-Stop-lox-LacZ* transgenic mice. In these mice, *Tie2-cre*–positive endothelial cells were irreversibly tagged with an expression of the *LacZ* transgene (Fig. 2*A*). Tumors of 1,000 mm^3 size were harvested and enzymatic β-galactosidase reaction was done in these tumors. *LacZ*-positive cells were marked by a blue precipitate in this assay. In addition to blue cells within vessels (endothelial cells), single blue cells were also found scattered throughout the tumor stroma (Fig. 2*B, black arrows*). To further identify the origin of such cells, we did double-labeling experiments using antibodies to β-galactosidase (*red*), FSP1 (*green*), and αSMA (*green*). The tissue was analyzed using

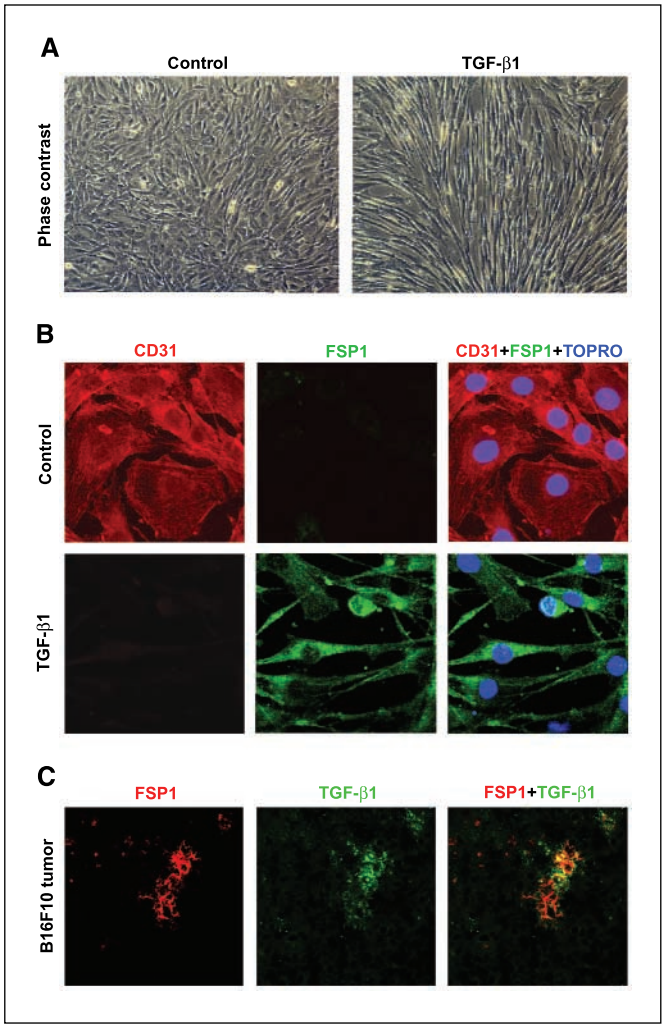

Figure 3. *A* and *B,* TGF-β1 induces EndMT involving MLEC *in vitro*. *A,* representative pictures of MLEC maintained in control medium for 48 h (*left*) or medium containing 10 ng/mL of TGF-β1 (*right*). *B,* representative photomicrographs of MLEC, which were labeled with antibodies to CD31 (*red*) and FSP1 (*green*). TGF-β1 induced an increase in the expression of FSP1 and a decrease in the expression of CD31. *C,* FSP1 and TGF-β1 double-labeling of B16F10 tumors. We stained B16F10 tumor tissues with antibodies to FSP1 (*red*) and TGF-β1 (*green*). Accumulation of $FSP1^+$ fibroblasts correlated with areas of intense TGF-β1 staining.

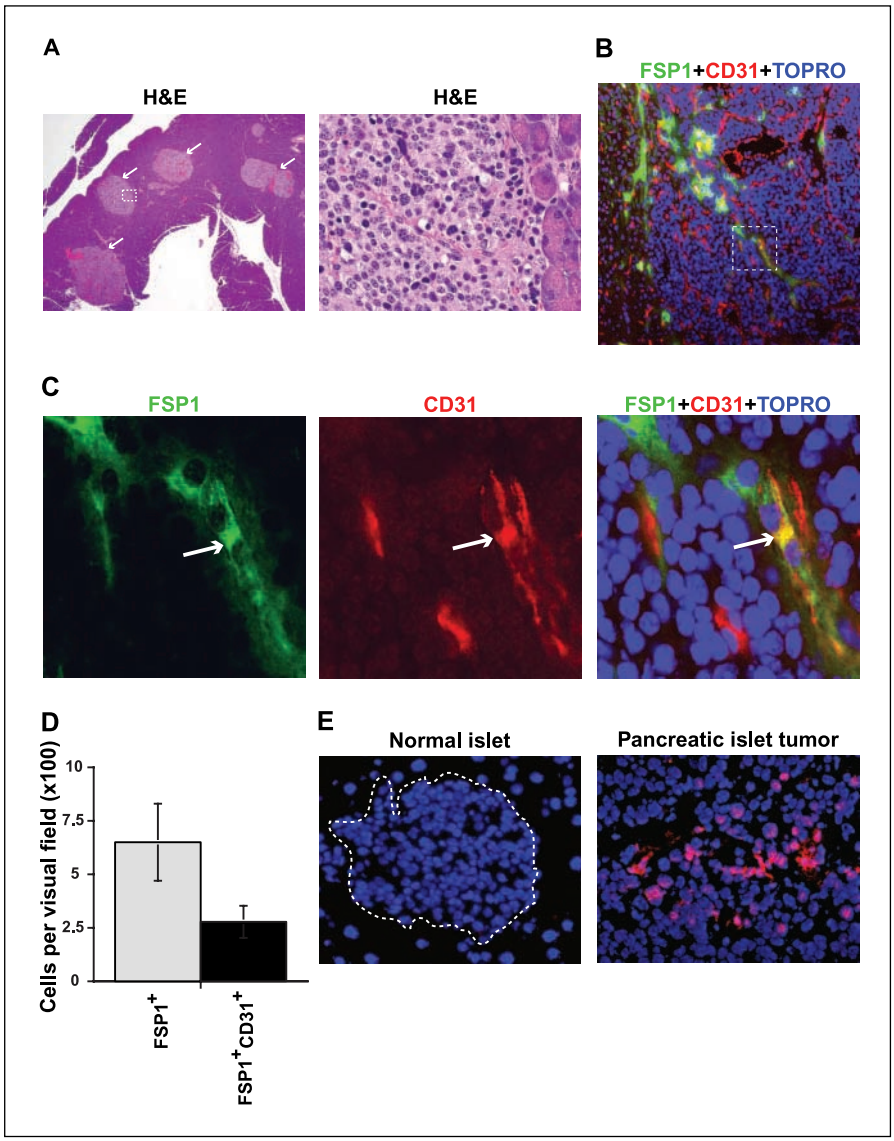

Figure 4. EndMT in Rip1-Tag2 tumors. *A,* pancreas tissue of Rip1-Tag2 transgenic mice was analyzed at an age of 13.5 wks. Representative photomicrographs of H&E-stained tissue sections. Original magnifications, ×4 (*left*) and ×60 (*right*). *Left,* angiogenic islet tumors (*arrows*); *right,* inset in (*B*). *B* and *C,* RIP1-Tag2 tumors were double-stained with antibodies to FSP1 (*green*) and CD31 (*red*). TOPRO-3 was used as a nuclear stain (*blue*). Representative pictures that were obtained with a confocal microscope. Original magnifications, ×20 (*B*) and ×100 (*C*). Inset in (*B*), the area that is displayed in (*C*) at a higher magnification. *Arrows,* $CD31^+FSP1^+$ cells. *D, columns,* number of all FSP1-positive cells (*empty column*) and FSP1/CD31 double-positive cells (*filled column*) per visual field. *E,* representative photomicrographs of a normal pancreatic islet (*left, dotted line*) and of a pancreatic islet tumor (*right*) labeled with antibodies to TGF-β1 (*red*). Original magnification, ×40.

confocal microscopy (Fig. 2*C* and *D*). Approximately 30% of the $FSP1^+$ cells in the tumor stroma were β-gal and FSP1 double-positive and 12% of the αSMA^+ cells revealed double positivity for αSMA and β-gal (Fig. 2*C* and *D*). Collectively, our studies provide a compelling genetic evidence for EndMT-derived CAF in the tumor microenvironment.

TGF-β1 induces EndMT in primary MLECs. TGF-β1 is a potent inducer of epithelial to mesenchymal transitions (14, 15). To further establish EndMT, we cultured and exposed primary MLECs to TGF-β1. Exposure to 10 ng/mL of TGF-β1 causes MLEC to acquire a spindle-shaped fibroblast-like morphology (Fig. 3*A*). Such phenotypic transitions are associated with a dramatic decrease in CD31 expression and an increase in FSP1 protein expression (Fig. 3*B*). Analysis of B16F10 tumor tissue with antibodies to FSP1 (*red*) and TGF-β1 (*green*) shows an accumulation of $FSP1^+$ cells in areas with the most intense TGF-β1 labeling (Fig. 3*C*), further providing causal support to the notion that TGF-β1 mediates EndMT within the tumor microenvironment.

Evidence for EndMT in the Rip1-Tag2 multistage carcinoma model. We used Rip1-Tag2 transgenic mice as a second tumor model to gain further insights into the occurrence of EndMT within the tumor microenvironment. In Rip1-Tag2 transgenic mice, the large T-antigen of SV40 is exclusively expressed in the β-cells of the excretory pancreas (16). In this cancer model, every mouse developed pancreatic islet tumors by 12 to 14 weeks of age (17). We harvested tumors from RIP1-Tag2 transgenic mice at the age of 13.5 weeks (advanced tumor burden; Fig. 4*A*) and did double-labeling experiments using antibodies to FSP1 and CD31 (Fig. 4*B* and *C*). Similar to B16F10 tumors, double-labeling experiments revealed a significant portion of $FSP1^+$ cells positive for both FSP1 and CD31, indicating EndMT as a mechanism for the recruitment of CAFs (Fig. 4*D*). Immunofluorescence labeling using primary antibodies to TGF-β1 confirmed the presence of TGF-β1 within the pancreatic islet tumor microenvironment (Fig. 4*E*).

Discussion

Solid tumors are a composite of cancer cells, endothelial cells, inflammatory cells, and fibroblasts (2). Although the relevance of fibroblasts in cancer progression is increasingly being recognized,

little is known about their origin (1). In this study, we provide evidence that endothelial cells contribute to the pool of CAFs via EndMT. Our previous studies have shown that CAF are a heterogeneous population (18). In this study, we use two different tumor models, *in vitro* EndMT assay and *Tie2-cre;R26Rosa-lox-Stop-lox-LacZ* transgenic mice, and we provide evidence that endothelial cells contribute to the accumulation of fibroblasts within the tumor microenvironment of angiogenic tumors. Our study also supports the notion that not all CAF are αSMA-positive and that $FSP1^+$ fibroblasts constitute a separate class of activated fibroblasts in the tumor microenvironment (18). The origin of activated fibroblasts and myofibroblasts is not exclusively via EndMT. Interestingly, fewer cells in our study colocalize with αSMA and CD31/LacZ compared with FSP1 and CD31/LacZ. Future studies will hopefully analyze many different mouse and human tumors to ascertain whether EndMT is a universal process in many cancers.

Several studies have shown the capacity of TGF-β1 in mediating epithelial to mesenchymal transition (11, 15). Cardiac endothelial cells undergo EndMT when exposed to TGF-β1, and cardiac fibrosis is associated with EndMT (13). In the present study, we show that TGF-β1–exposed lung endothelial cells could undergo EndMT. We propose that endothelial cells under the influence of autocrine and paracrine TGF-β1 (abundantly present in many tumors; refs. 19, 20), undergo EndMT. Our use of tumors grown in *Tie2-cre;R26Rosa-lox-Stop-lox-LacZ* transgenic mice provides compelling proof that endothelial cells are capable of acquiring mesenchymal transition. Collectively, our study provides evidence that EndMT is an important source for the accumulation of cancer-promoting CAFs.

Acknowledgments

Received 8/16/2007; revised 9/7/2007; accepted 9/25/2007.

Grant support: Research grants DK62987 (R. Kalluri), DK55001 (R. Kalluri), DK61688 (R. Kalluri), AA013913 (R. Kalluri), Ruth L. Kirschstein National Research Service Award F32 HL082436-01 (E. Zeisberg), and a Mentored Clinical Scientist Development Award K08 DK074558-01 (M. Zeisberg) from the NIH; the ASN Carl W. Gottschalk Scholar grant (M. Zeisberg) and research funds from the Beth Israel Deaconess Medical Center for the Division of Matrix Biology.

The costs of publication of this article were defrayed in part by the payment of page charges. This article must therefore be hereby marked *advertisement* in accordance with 18 U.S.C. Section 1734 solely to indicate this fact.

References

1. Kalluri R, Zeisberg M. Fibroblasts in cancer. Nat Rev Cancer 2006;6:392–401.
2. Hanahan D, Weinberg RA. The hallmarks of cancer. Cell 2000;100:57–70.
3. Tlsty TD, Hein PW. Know thy neighbor: stromal cells can contribute oncogenic signals. Curr Opin Genet Dev 2001;11:54–9.
4. Elenbaas B, Weinberg RA. Heterotypic signaling between epithelial tumor cells and fibroblasts in carcinoma formation. Exp Cell Res 2001;264:169–84.
5. Dvorak HF. Tumors: wounds that do not heal. Similarities between tumor stroma generation and wound healing. N Engl J Med 1986;315:1650–9.
6. Koni PA, Joshi SK, Temann UA, Olson D, Burkly L, Flavell RA. Conditional vascular cell adhesion molecule 1 deletion in mice: impaired lymphocyte migration to bone marrow. J Exp Med 2001;193:741–54.
7. Mao X, Fujiwara Y, Orkin SH. Improved reporter strain for monitoring cre recombinase-mediated DNA excisions in mice. Proc Natl Acad Sci U S A 1999;96:5037–42.
8. Hamano Y, Zeisberg M, Sugimoto H, et al. Physiological levels of tumstatin, a fragment of collagen IV α3 chain, are generated by MMP-9 proteolysis and suppress angiogenesis via αvβ3 integrin. Cancer Cell 2003;3:589–601.
9. Maeshima Y, Sudhakar A, Lively JC, et al. Tumstatin, an endothelial cell-specific inhibitor of protein synthesis. Science 2002;295:140–3.
10. Zeisberg M, Bonner G, Maeshima Y, et al. Renal fibrosis: collagen composition and assembly regulates epithelial-mesenchymal transdifferentiation. Am J Pathol 2001;159:1313–21.
11. Zeisberg M, Hanai J, Sugimoto H, et al. BMP-7 counteracts TGF-β1-induced epithelial-to-mesenchymal transition and reverses chronic renal injury. Nat Med 2003;9:964–8.
12. Zeisberg EM, Ma Q, Juraszek AL, et al. Morphogenesis of the right ventricle requires myocardial expression of Gata4. J Clin Invest 2005;115:1522–31.
13. Zeisberg EM, Tarnavski O, Zeisberg M, et al. Endothelial-to-mesenchymal transition contributes to cardiac fibrosis. Nat Med 2007;13:952–61.
14. Kalluri R, Neilson EG. Epithelial-mesenchymal transition and its implications for fibrosis. J Clin Invest 2003;112:1776–84.
15. Thiery JP, Sleeman JP. complex networks orchestrate epithelial-mesenchymal transitions. Nat Rev 2006;7:131–42.
16. Hanahan D. Heritable formation of pancreatic β-cell tumours in transgenic mice expressing recombinant insulin/simian virus 40 oncogenes. Nature 1985;315:115–22.
17. Bergers G, Brekken R, Mcmahon G, et al. Matrix metalloproteinase-9 triggers the angiogenic switch during carcinogenesis. Nat Cell Biol 2000;2:737–44.
18. Sugimoto H, Mundel TM, Kieran MW, Kalluri R. identification of fibroblast heterogeneity in the tumor microenvironment. Cancer Biol Ther 2006;5:1640–6.
19. Bierie B, Moses HL. TGF-β and cancer. Cytokine Growth Factor Rev 2006;17:29–40.
20. Akhurst RJ. TGF β signaling in health and disease. Nat Genet 2004;36:790–2.